Journal of Physics: Conference Series **759** (2016) 012020 doi:10.1088/1742-6596/759/1/012020

Energetics of dendrimer binding to HIV-1 gp120-CD4 complex and mechanismic aspects of its role as an entry-inhibitor

Suman Saurabh, Anil Kumar Sahoo and Prabal K. Maiti

Center for Condensed Matter Theory, Indian Institute of Science, Bangalore 560012, Karnataka, India

E-mail: maiti@physics.iisc.ernet.in

Abstract. Experiments and computational studies have established that de-protonated dendrimers (SPL7013 and PAMAM) act as entry-inhibitors of HIV. SPL7013 based Vivagel is currently under clinical development. The dendrimer binds to gp120 in the gp120-CD4 complex, destabilizes it by breaking key contacts between gp120 and CD4 and prevents viral entry into target cells. In this work, we provide molecular details and energetics of the formation of the SPL7013-gp120-CD4 ternary complex and decipher modes of action of the dendrimer in preventing viral entry. It is also known from experiments that the dendrimer binds weakly to gp120 that is not bound to CD4. It binds even more weakly to the CD4-binding region of gp120 and thus cannot directly block gp120-CD4 complexation. In this work, we examine the feasibility of dendrimer binding to the gp120-binding region of CD4 and directly blocking gp120-CD4 complex formation. We find that the process of the dendrimer binding to CD4 can compete with gp120-CD4 binding due to comparable free energy change for the two processes, thus creating a possibility for the dendrimer to directly block gp120-CD4 complexation by binding to the gp120-binding region of CD4.

1. Introduction

The entry of HIV into target $CD4^+$ T cells in humans is initiated by the binding of the viral surface protein gp120 to the target cell receptor protein CD4 [1]. This binding induces structural changes in gp120, which help it bind to the target cell trans-membrane protein CCR5 or CXCR4 leading to further conformational changes resulting in membrane fusion. The disruption of binding between the proteins that facilitate viral entry is one of the many drug-discovery strategies aimed at developing an HIV inhibitor. Small molecule drugs like maraviroc, which blocks binding of gp120 to CCR5 (second stage in the entry process), utilize such a strategy [2]. While the swift resistance mechanism of the virus renders individual drugs incapable of performing their pre-defined function after a brief period of use, the search for a drug with a large genetic barrier to resistance is still on.

Dendrimers are highly branched polymers. They consist of a core, a branching unit and terminal groups [3]. Among many families of dendrimer molecules, SPL7013 and PAMAM dendrimers are experimentally known to exhibit anti-retroviral activity [4]. Time-of-addition experiments indicate that these dendrimers act as entry inhibitors [5]. The multivalent nature of the dendrimer allows it to bind in multiple possible conformations with various bio-molecules.

Unlike small molecule drugs, which bind to the cavities on protein surfaces, the dendrimer, being a large molecule, can bind a protein over a very large contact area. Although there is no specific binding conformation, the huge loss in entropy due to dendrimer binding imparts partial specificity to the binding process. SPL7013 is thought to act via different mechanisms on different viral strains (R5, X4 and R5X4). In a recent computational study of the stability of R5 HIV-1 gp120-CD4 complex in the presence of SPL7013, we have elucidated the potential mechanism of its action against R5 viruses, which was previously unknown [6]. The dendrimer destabilizes the gp120-CD4 complex by docking to R5 gp120, allosterically breaking many key gp120-CD4 contacts and in the process helping preclude viral entry. A similar effect of the PAMAM dendrimer on the gp120-CD4 complex was observed in another computational study [7], where the binding energy of the complex was found to decrease drastically in the presence of the dendrimer.

The HIV-1 gp120 is structurally complex. It has two main domains (inner and outer) connected by a bridging sheet (see Figure 1). The protein also contains fluctuating loops which produce a constantly moving target for the immune system, enabling the virus to evade human immune responses.

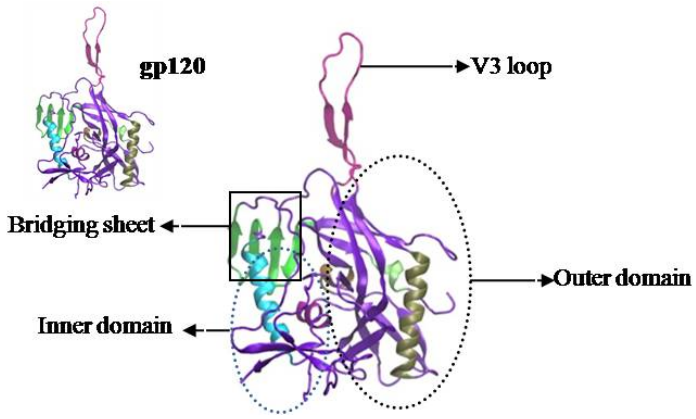

Figure 1. Structure of gp120 (top view), with different regions labeled. The black and blue ellipses highlight the outer and inner domains respectively. The rectangle covers the bridging sheet (β-sheets in green). V3 loop is shown as the extended structure (mauve).

gp120 binds to CD4 with low affinity. The CD4 binding region of gp120 contains many unstructured loops. Thus the huge enthalpy of binding ($\sim$ -62 kcal/mol) [8] is offset by the large loss in entropy ($\sim$ -53 kcal/mol) [8]. The dendrimers further destabilize the complex and prevent the formation of the number of gp120-CD4 complexes necessary for viral entry.

In this work, we study the molecular details of SPL7013-gp120-CD4 ternary complex, using molecular docking, equilibrium simulations and binding energy calculations. We focus on the V3 loop and study various effects of its strong positive charge on dendrimer-gp120 binding. We also aim at verifying the experimental findings regarding the mechanism of action of SPL7013. The dendrimer when docked to gp120-CD4 complex binds to gp120. In our previous study [6] we found that when the dendrimer docked to gp120 in the absence of CD4, there were only a few low ranked docking output conformations from ZDOCK [9] wherein SPL7013 was bound to the CD4-binding region of gp120. We showed that the binding energy of such binding conformations is very low compared to the one where SPL7013 binds to the V3 loop of gp120. This shows that the dendrimer cannot prevent gp120-CD4 binding by blocking the CD4 binding region of gp120. That SPL7013 binds weakly to R5 gp120 compared to the gp120-CD4 complex is known [6]. When, in experiments, R5 HIV-1 was exposed to SPL7013 and then used to infect cells in the absence of the dendrimer, the dendrimer was found to be inefficacious in preventing viral entry. Whereas the dendrimer was very effective with R5 HIV-1 when present in culture with the virus and target cells. This indicates two possible mechanisms for the dendrimer to stop gp120 from binding to CD4. Firstly, the dendrimer can bind to gp120 in complex with CD4 and

allosterically hinder their complexation by breaking key contacts. Secondly, before gp120-CD4 complexation occurs, it can bind to the region of CD4 that goes into the CD4-binding cavity of gp120 in the gp120-CD4 complex (the gp120-binding region of CD4) and block their binding. Although the first possibility is well explored and is energetically feasible, the feasibility of the second possibility has not been studied. Here, we study the energetics and consequent feasibility of the second option.

2. Materials and Methods

2.1. Building the SPL7013 dendrimer

The SPL7013 dendrimer was built using Dendrimer Builder Toolkit (DBT) [10] developed some years back in our laboratory. The core, repeating units and terminal residues were designed as per the chemistry and topology of the dendrimer. All the residues with cap(s) were optimized using GAUSSIAN03 [11] with the HF/6-31+G (d,p) basis set. Restrained electrostatic potential (RESP) [12] charges were calculated using Antechamber module [13] of AMBER. During RESP calculation, cap charges were set to zero. The net charge on the core and repeating residues were also set to zero. To have the anionic form, we set the charge on the terminal de-protonated residue to be -2. Post optimization and RESP charge calculation, the caps were removed from the residues using xleap module in AMBER. The de-capped residues thus obtained were used for building the SPL dendrimer of different generations using DBT. The optimized structure of generation 4 (G4) SPL7013 dendrimer was thus obtained.

2.2. MD simulations of individual molecules

We used the AMBER12 [14] software package with GAFF [15] set of parameters for the SPL7013 G4 dendrimer. The dendrimer was solvated with TIP3P water model with a 13 Å hydration shell in all three directions using the xleap module. Additionally, 64 Na^+ ions were added to make the system charge neutral.

For the gp120-CD4 complex, we have used the crystal structure of the YU2 gp120 core complexed with CD4 and a functionally sulfated antibody F12d (PDB id: 2QAD) [16]. The antibody was removed from the crystal structure to get the initial 3-D model of the gp120-CD4 complex. The complex was solvated using TIP3P model of water using xleap module of AMBER12 [14]. 9 Cl^- ions were also added to make the solvated gp120-CD4 system charge neutral. The system contained 275726 atoms with 89310 water molecules and 9 Cl^- ions.

Similarly, to study the CD4 structure, we removed both gp120 and the F12d antibody and obtained the structure of monomeric CD4. The structure was solvated in TIP3P water with a water buffer of 30 Å in the x- and y-directions and 15 Å in the z-direction. The solvated system was then neutralized by adding 4 Cl^- ions using xleap.

We have used ff99SB parameters [17] to describe inter and intra-molecular interactions corresponding to the proteins. Ions were described using the Joung-Cheatham parameter set [18]. All the above three systems namely solvated SPL system, solvated gp120-CD4 complex as well as solvated CD4 system were energy minimized using the following protocol: we first performed 1000 steps of steepest descent minimization. This was followed by another 2000 steps of conjugate gradient minimization. During the minimization, the solute atoms were fixed to their initial co-ordinates using harmonic constraints with a force constant of 500 kcal/mol/$Å^2$ while the water molecules were allowed to reorganize and eliminate unfavorable contacts with the solute. The systems were further subjected to 5000 steps of conjugate gradient minimization, with the harmonic constraints on the solute going from 20 kcal/mol/$Å^2$ to 0 with a reduction of 5 kcal/mol/$Å^2$ every 1000 steps. After minimization the systems were gradually heated from 0 to 300K during a 40 ps long MD simulation. During heating, the solute atoms were restrained to their initial position with a force constant of 20 kcal/mol/$Å^2$, which allowed slow relaxation of the solute. SHAKE method [19] was use for constraining bonds involving hydrogen with a

geometrical tolerance of 5 x 10^{-4} Å. This allowed the use of a 2 fs time step. The long range electrostatic interactions were handled with the Particle Mesh Ewald (PME) method. The real space cut-off was set to 9 Å. Finally, the dendrimer was subjected to 82 ns long NPT simulation. While for the protein systems, a 500 ps long NPT run was performed followed by 100 ns and 60 ns long NVT runs for gp120-CD4 complex and monomeric CD4 respectively. The resulting structures of CD4 and the gp120-CD4 complex were employed for further docking and simulation studies.

2.3. Docking of SLP7013 to CD4 and to the gp120-CD4 complex

ZDOCK [9], an automated protein docking server, was used for docking the gp120-CD4 complex and the de-protonated SPL7013 dendrimer. ZDOCK uses a scoring function which is based on sum of scores from electrostatics, surface complementarity and desolvation energy. Desolvation energy is defined as the energy required for breaking two amino acid-water bonds and forming two amino acid-amino acid bonds. The gp120-CD4 complex after 40 ns of MD simulation in the NVT ensemble and the dendrimer after 80 ns of MD simulation in the NPT ensemble (see above) were employed as the receptor and the ligand, respectively, for docking. We also employed several other structures of the dendrimer between 70 and 80 ns of MD simulation to examine the robustness of our findings towards the initial structures employed, and found very similar docking conformations. The input parameters were kept at their default values in ZDOCK. Of the resulting docked structures, we considered the top 8 for further analysis.

We repeated a similar procedure with monomeric CD4 (using structures after 16 ns, 20 ns and 50 ns of MD simulation docked to 45 ns, 60 ns and 80 ns dendrimer structures respectively) as receptor and found that almost all of the docking outputs had the dendrimer bound to the region of CD4 that goes into the CD4 binding site of gp120 in the gp120-CD4 complex. We selected one conformation out of the top ten ZDOCK predictions for each input receptor-ligand pair. The three selected CD4-SPL7013 complexes were further used for equilibrium simulations and energy calculations.

2.4. MD simulation and energetics of docked structures

Even though ZDOCK assigns ranks based on a sophisticated scoring function, in light of the CAPRI test runs, where ZDOCK predicted correct binding poses for only half of the targets used in the study, it is important to check whether ZDOCK ranked the complexes correctly. Accordingly, we performed MD simulations of the top 8 SPL7013-gp120-CD4 docked structures to compute their binding energies and examine their stability.

Each of the docked structures was immersed in a water box (with at least a 30 Å water layer in all the three directions). 64 Na^+ ions and 9 Cl^- ions were added for charge neutrality. The structures were allowed to equilibrate and were subjected to 60 ns or more of MD simulation in an NVT ensemble. The binding energy between gp120-CD4 (receptor) and the dendrimer (ligand) was then calculated using the MMGBSA [20] module of AMBER12. Entropy calculations were also performed using normal mode analysis (see below). From the binding energy calculations, we found that the highest ranked ZDOCK structure was not the most stable. We re-ranked the ZDOCK outputs based on our energy calculations. In the text we will mention the complexes according to their energy ranks (complex 1 to complex 8). We extended the NVT runs for complexes 1, 3, and 8 to a total of 100 ns. The structures of the ternary complexes studied in this work are shown at appropriate places in the text.

For CD4-SPL7013 docking, the SPL7013 docks near the gp120-binding region of CD4 for majority of the ZDOCK generated structures (28 out of 30 structures). We selected three structures with considerably different binding conformations (see Results and Discussion). These systems were solvated in TIP3P water box with a buffer of 33 Å in the x- and y- directions and 13 Å in the z-direction. 64 Na^+ ions and 4 Cl^- ions were added for charge neutralization. The

resulting solvated structures were first energy minimized using the same protocol as described above, after which a 500 ps long NPT simulation was performed followed by a 50 ns long NVT simulation.

2.5. Calculation of binding free energy of various complexes

We used the MMGBSA method employed in the MMPBSA.py [20] module of AMBER12 [14] to calculate the binding free energy of various binary and ternary complexes. The free energy is computed as ΔG=ΔE_{bind}-TΔS_{bind}, where the binding enthalpy, ΔE_{bind}=ΔE_{ele}+ΔE_{vdw}+ΔE_{int}+ΔE_{sol} consists of changes in the electrostatic energy, ΔE_{ele}, van der Waals energy, ΔE_{vdw}, the internal energy from bonded terms, ΔE_{int}, and the solvent contribution, ΔE_{sol}. The latter contribution, ΔE_{sol}=ΔE_{es}+ΔE_{nes}, is the sum of the electrostatic energy, ΔE_{es}, calculated using the Generalized Born (GB) method, and the non-electrostatic energy, ΔE_{nes}, given by γSASA+β, (γ = 0.00542 kcal/Å^2 is the surface tension, β = 0.92 kcal/mol, and SASA is the solvent-accessible surface area of the molecule [21]). We performed similar calculations to estimate the binding energies of CD4-SPL7013 complexes.

Binding entropy was also calculated for all the complexes. Rotational and translational entropies were calculated by considering the receptor and ligand as rigid rotors. Harmonic approximation was employed. The use of rigid rotor model enables the use of a reduced Hessian (6X6) that needs to be diagonalized. The vibrational term was calculated using normal mode analysis which also uses harmonic approximation for entropy calculation. This method requires the diagonalization of the full fledged Hessian (3N X 3N, N being the number of atoms) for determination of the normal modes.

3. Results and Discussion

3.1. Energetics of dendrimer binding to gp120-CD4 complex

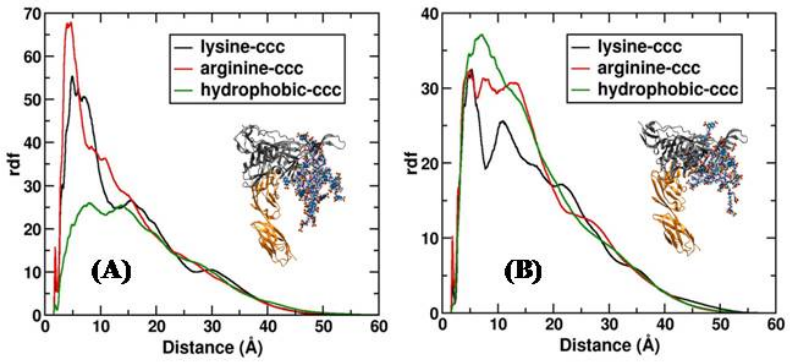

Figure 2. (A) and (B) Distribution of the terminal aromatic groups of SPL dendrimer (ccc) around the charged and hydrophobic residues of two different dendrimer binding conformations corresponding to complex 1 and complex 3 respectively. The distribution has been calculated around the charged and hydrophobic residues that form atomic contacts with the dendrimer. The ternary complexes are shown in the inset.

The SPL7013 dendrimer has naphthalene disulphonic acid based anionic aromatic residue as the terminal group [6]. The dendrimer interacts with gp120 mainly through electrostatic and hydrophobic interactions. The dendrimer binds to gp120 in a manner in which the interactions of the terminal groups are optimally satisfied. We plot (see Figure 2) the radial distribution of the terminal groups (named ccc) around positively charged and hydrophobic residues of gp120 which

form contacts with the dendrimer in case of complex 1 and complex 3. We find that the terminal groups of the dendrimer are placed very close to the positively charged residues of gp120 (∼5 Å), whereas the average distance from the hydrophobic residues is a bit larger (∼7.5 Å) and the corresponding peaks are smaller than those corresponding to the positively charged residues. On closer observation we find that the terminal rings are oriented with their planes parallel to the guanidinium groups of arginine. Such stacking interaction between aromatic rings and the basic residues is well known in literature [22,23] and provides stability over and above the long-range electrostatic interaction. We have also calculated the residue-wise energy contributions to the protein-dendrimer binding energy for complex 1 and complex 3 corresponding to various gp120 residues that form atomic contacts with the dendrimer (see Figure 3). Atomic contacts were defined to exist when an atom of a gp120 residue fell within 3 Å of an atom belonging to the dendrimer. We observe that the ARG and LYS residues have the largest negative contribution to the total binding energy (see Figure 3(A) and (B)). In case of complex 1, ARG-142, LYS-143, ARG-151, LYS-172, ARG-239, ARG-267 and ARG-271 provide large stabilization to the ternary complex. In case of complex 3, LYS-45, ARG-142, LYS-143, ARG-151, ARG-164, ARG-246 and ARG-267 have large contributions to the stability of the ternary complex. We also see that in case of complex 3 GLU-156 has a significant positive contribution to the binding energy owing to its negative charge. All this shows that the electrostatic interaction plays a dominant role in the binding of the dendrimer to the gp120-CD4 complex and the binding poses for the complex are arrived at with a priority to electrostatic considerations.

The V3 loop of gp120 plays a very important role in stabilizing the SPL7013-gp120-CD4 complex. The base of the V3 loop is a region of very high positive charge density and the poly-anionic dendrimer can gain large electrostatic stabilization by choosing to bind around this region. In Figure 3(C), we show the positions of the positively charged residues that have large contributions to the stability of the ternary complexes 1 and 3. We observe that all these residues lie on the V3 loop, near the V3 loop base and the bridging sheet. We performed a simulation with the dendrimer initially placed at a center of mass distance of 50 Å from gp120 in complex with CD4. When the system was time evolved, we found that the dendrimer very quickly approached gp120 and docked on the V3 loop as shown in Figure 4(A). For the SPL7013-gp120-CD4 ternary complexes with initial docking position of SPL7013 away from V3 loop (complex 7 and 8), the dendrimer was found to move towards the V3 loop during the course of the simulation. We calculated the binding energy between gp120-CD4 and the dendrimer for complex 7 at different stages of the simulation and found that as the dendrimer approaches the V3 loop, the binding energy increases significantly (see Figure 4(B)). This highlights the importance of the V3 loop region of gp120 in dendrimer binding and suggests that if the virus attains mutations in this region, it would significantly affect the efficacy of the dendrimer.

3.2. Dendrimer destabilizes gp120-CD4 complex by inducing binding-position dependent conformational changes into gp120

It is known from earlier studies that the dendrimer binds to gp120 in the gp120-CD4 complex and disrupts key contacts between the two proteins by modifying the conformation of gp120 [6]. In this section we show that the manner and degree of conformational change induced in gp120 depends mainly on the position of dendrimer binding, and so does the degree of destabilization of the gp120-CD4 complex. Unlike small drug molecules, which bind to specific binding pockets on the target protein, dendrimer can bind at different positions, engage a large number of gp120 residues in the binding process and thus is expected to have a huge genetic barrier to resistance, which is a key property of a robust drug. In our earlier work, we studied the effect of dendrimer binding on the conformation of gp120 for complex 3 [6]. We found that the dendrimer induces a significant global tilt in gp120 with respect to CD4. In addition to that, it physically forms contacts with the residues on the bridging sheet near the CD4 binding site and through

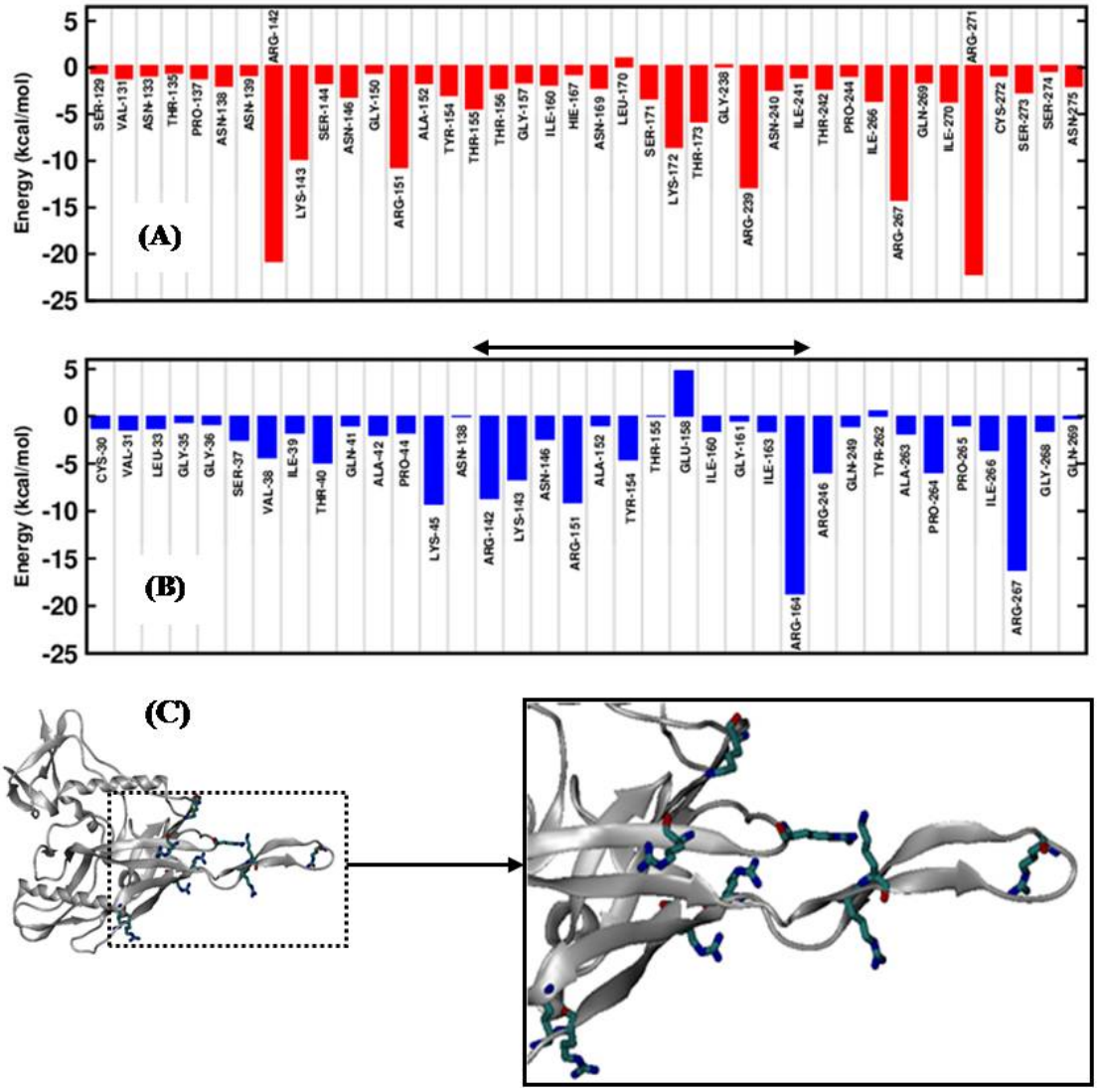

Figure 3. (A) The residue-wise contributions corresponding to various gp120 residues to the dendrimer-protein binding energy for complex 1. (B) The residue-wise contributions corresponding to various gp120 residues to the dendrimer-protein binding energy for complex 3. The residues belonging to V3 loop in case of complex 3 are marked on the x-axis. (C) Locations of positively charged residues of gp120 that have a large energy contribution to the binding of the dendrimer to gp120-CD4 complex.

electrostatic interactions, pulls various gp120 residues out of the contact of CD4. To show that the dendrimer can actually cause the disruption in contacts in multiple ways, we study the effect of the dendrimer on complex 8 with the dendrimer binding exactly on top of the V3 loop, as shown in Figure 5. In our previous study [6] we had found that complex 3 and complex 8 showed significant reduction in gp120-CD4 binding energy as compared to the gp120-CD4 binary complex in the absence of the dendrimer.

First thing to notice is that there is no relative tilt in this case as was seen for complex 3 (see Figure 5). So the tilt was a result of a particular dendrimer binding position. The most

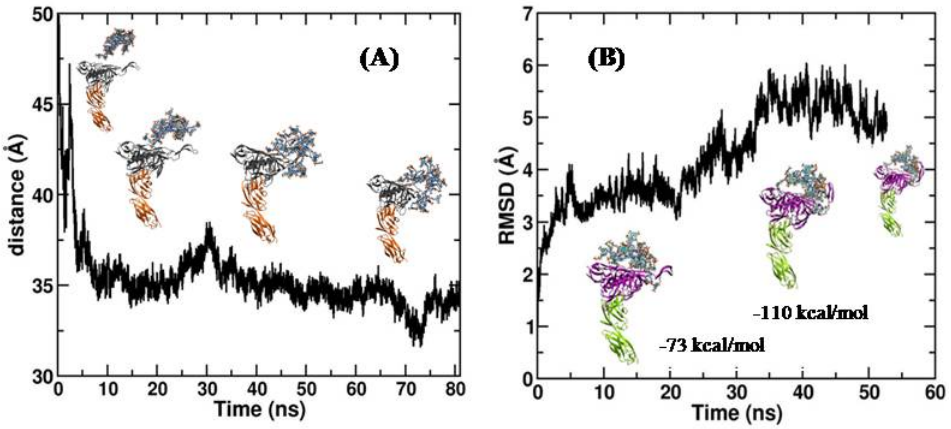

Figure 4. (A) Time evolution of the distance between gp120 and the dendrimer initially placed 50 Å apart along with snapshots at various times. The dendrimer approaches gp120 and attaches to the V3 loop. (B) RMSD of complex 7 with respect to the minimized structure. The figures in the insets show the conformation of complex 7 at various stages of the simulation. One can clearly see how the dendrimer shows displacement towards the V3 loop.

significant difference between the structure without dendrimer and the structure of complex 8 is in the conformation of the V3 loop with respect to the other domains of gp120. It is well known that the V3 loop acts as an electrostatic modulator of gp120 conformation [24] and thus the conformation of gp120 will strongly depend on the conformation of the V3 loop. By freezing

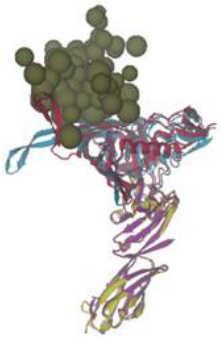

Figure 5. Conformational changes in gp120-CD4 complex on dendrimer binding. The structures corresponding to the average of 400 conformations corresponding to the last 4 ns of MD trajectory of complex 8 (red and yellow) and no dendrimer (blue and mauve) simulation superposed with the CD4 structures aligned. The difference in orientations of the V3 loop is clearly visible. The position of the dendrimer is shown in the beads representation on the red gp120.

the V3 loop in an unusual orientation, the dendrimer would induce conformational changes in other regions of gp120, like the bridging sheet and hence would affect gp120-CD4 binding. So, in case of complex 8 the dendrimer does not disrupt gp120-CD4 binding by physically pulling gp120 residues out of the influence of CD4. It does so by unusually deforming the V3 loop which in-turn induces conformational changes in gp120. The comparison of the mode of action of the dendrimer for complexes 3 and 8 indicate that the dendrimer can act in a number of different ways to disrupt the gp120-CD4 complex, depending on its binding position on gp120. Thus the virus may not be able to escape the entry-inhibitory property of the dendrimer by undergoing mutations that destabilize a particular binding conformation of the dendrimer as there will always be an alternative dendrimer binding conformation that can still destabilize the gp120-CD4 complex.

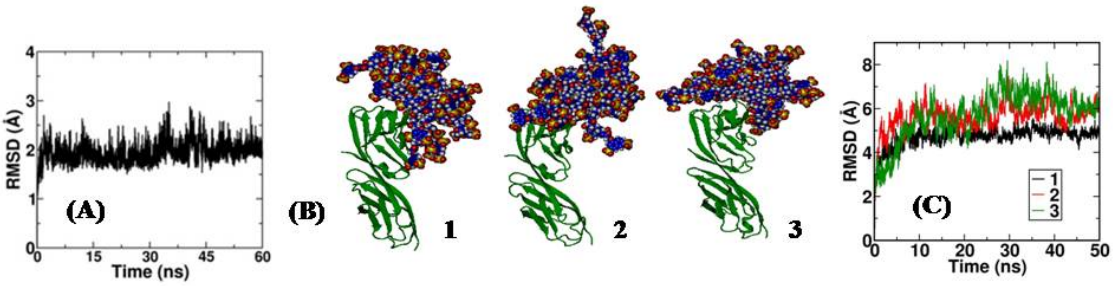

Figure 6. (A) RMSD of CD4 through the 60 ns long MD simulation. The starting conformation of CD4 was obtained by removing gp120 from the gp120-CD4 structure obtained after 40 ns of MD simulation. The RMSD saturates starting from a very early stage in the production run. (B) The starting conformations of the three CD4-SPL7013 docked structures used for MD simulations and energy calculations. (C) RMSD for the three CD4-SPL7013 complexes shown in (B) with respect to their minimized structure.

3.3. Dendrimer binding to CD4

In this section, we study the feasibility of SPL7013 binding to the gp120-binding region of CD4. In an earlier study, we docked the dendrimer to the gp120-CD4 binary complex and found that almost all the docking predictions had the dendrimer bound to gp120, while there were no predictions with the dendrimer bound to CD4 [6]. We performed simulations with gp120-SPL7013 complexes in the absence of CD4 and found that the dendrimer binding to gp120 is much weaker than its binding to the gp120-CD4 complex [6]. The binding energies suggested that the dendrimer could not block gp120-CD4 complexation by sterically blocking the CD4 binding region of gp120. Here, to check the feasibility of SPL7013 binding to CD4 and blocking its binding to gp120, we removed gp120 from the gp120-CD4 complex obtained after 40 ns of MD simulation, and simulated the resulting CD4 molecule for 60 ns using the protocol described in the Materials and Methods section. The RMSD for the CD4 structure seemed to saturate very early during the course of the simulation at a value in the range of 2-2.5 Å (see Figure 6 (A)). We extracted three different CD4 structures along the MD trajectory and docked them with three different dendrimer structures, obtained from the 80 ns long NPT simulation of the dendrimer (see Materials and Methods). Surprisingly, for the three different CD4 structures extracted from different stages of the MD trajectory, docked to three different dendrimer conformations, we found that almost all the top 10 structures predicted by ZDOCK had the dendrimer bound to the gp120-binding region of CD4. To estimate the binding energy between CD4 and SPL7013, with an aim to establish whether the dendrimer can utilize its binding to CD4 for blocking viral entry, we selected three CD4-SPL7013 binary complexes among the ZDOCK output structures. The selected structures are shown in Figure 6(B). The three complexes have considerably different binding conformations. We performed 50 ns long MD simulations of the three binary complexes (RMSDs shown in Figure 6(C)), and performed binding energy calculations using MMPBSA module of AMBER12 [14]. The results from the binding energy calculation are shown in Table 1 along with a comparison with other complexes.From the data in Table 1 we see that the binding energy (BE) for the gp120-CD4 complex (-62 kcal/mol) is much larger than the BE between gp120 and SPL7013 (-41 kcal/mol), with the dendrimer bound to gp120 at its CD4-binding region. The entropy of binding for the gp120-CD4 complex is -53 kcal/mol which gives a binding free energy (ΔF_{avg}) of -9 kcal/mol. As the free dendrimer constitutes a strongly fluctuating system, the entropy loss when the dendrimer binds to gp120 is expected to be huge.

Table 1. Average free energy of binding for various complexes. (All energies are reported in kcal/mol.)

	gp120-CD4	SPL7013-(gp120-CD4) (V3 loop)	gp120-SPL7013 (V3 loop)	gp120-SPL7013 (CD4-binding region)	CD4-SPL7013 (gp120-binding region)
BE	-62±3 [8]	-136±10 [6]	-99±10 [6]	-41±25 [6]	-75±9.
$T\Delta S$	-53±3 [8]	-96±9 [6]	–	–	-61±6.
ΔF_{avg}	-9 kcal/mol	-40 kcal/mol	–	–	-14 kcal/mol.

The gp120-SPL7013 complex with SPL7013 bound to the CD4-binding region of gp120 is thus expected to be unstable. So, thermodynamically, gp120 would prefer to bind CD4 than to bind SPL7013 at its CD4-binding region. In contrast, the ΔF_{avg} for CD4-SPL7013 complex (-14 kcal/mol, averaged over the three complexes studied), with the dendrimer binding at the gp120-binding region of CD4 is comparable to that for the gp120-CD4 complex. These two processes can thus compete with each other. Hence, in an experimental mixture of the target cells, virions and dendrimer, the dendrimer and gp120 would compete with each other to bind CD4. Thus, the calculation suggests that the dendrimer can block gp120-CD4 complexation by binding to CD4 at its gp120-binding region and sterically hindering the process. As entropy is expected to play a very important role, a more accurate calculation of the entropy of binding can establish this on a firmer basis as a parallel mechanism of entry-inhibition by the SPL7013 dendrimer.

4. Conclusion

In this work we study the molecular level energetics of the process of the dendrimer binding to the HIV-1 gp120-CD4 complex. Through residue-level energy calculations, we find that the V3 loop region has a major contribution to the binding and the complexation is driven by electrostatics. We also find that the dendrimer utilizes a large number of gp120 residues for binding. Drug evasion by the virus would require it to mutate at multiple sites. Such large scale mutations may induce significant conformational changes in gp120, rendering it incapable of inducing viral entry. In addition to this, the dendrimer can affect gp120-CD4 binding in multiple ways. For different positions at which it binds the gp120-CD4 complex, it disrupts a different set of contacts. Thus mutations that hinder a particular binding pose may not be sufficient for the virus to dodge the dendrimer. We also studied the binding between CD4 and SPL7013 and deduced through end-state energy calculations that the process of the dendrimer binding to CD4 may energetically compete with gp120-CD4 binding, in the process, sterically blocking gp120 from binding CD4. The validity of this finding needs to be confirmed by experiments.

Acknowledgments

This work was funded by the DST Mathematical Biology Initiative at the Indian Institute of Science, Bangalore.

References

[1] Chan D C and Kim P S 1998 *Cell* **93** 681-84
[2] MacArthur R D and Novak R M 2008 *Clin. Infect. Dis.* **47** 236-41
[3] Maiti P K, Cagin T, Wang G and Goddard W A 2004 *Macromolecules* **37** 6236-54
[4] Jiminez J L, Pio M, Mata F J, Gomez R, Munoz E, Leal M and Munoz-Fernandez M 2012 *New J. Chem.* **36** 299-309
[5] Tyssen D *et al.* 2010 *PLos One* **5** e12309

[6] Nandy B , Saurabh S, Sahoo A K, Dixit N M and Maiti P K 2015 *Nanoscale* **7** 18628-41
[7] Nandy B, Bindu D H, Dixit N M and Maiti P K 2013 *J. Chem. Phys.* **139** 024905
[8] Myszka D G, Sweet R W, Hensley P, Brigham-Burke M, Kwong P D, Hendrickson W A, Wyatt R, Sodroski J and Doyle M L 2000 *Proc. Natl. Acad. Sci. USA* **97** 9026-31
[9] Chen R, Li L and Weng Z 2003 *Proteins* **52** 80-87
[10] Chan D C, Kim P S, Maingi V, Jain V, Bharatam P V and Maiti P K 2012 *J. Comput. Chem.* **33** 1997-2011
[11] Frisch M J *et al.* 2004 *Gaussian03 Revision C.02* (Wellington CT: Gaussian Inc.)
[12] Bayly C I, Cieplak P, Cornell W D and Kollman P A 1993 *J. Phys. Chem.* **97** 10269-80
[13] Case D *et al.* 2012 *AMBER12* (San Fransisco: University of California)
[14] Wang J, Wang W, Kollman P A and Case D A 2006 *J. Mol. Graphics Modell.* **25** 247260
[15] Wang J, Wolf R M, Caldwell J W, Kollman P A and Case D A 2004 *J. Comput. Chem.* **25** 1157-74
[16] Huang C C *et al.* 2007 *Science* **317** 1930-34
[17] Hornak V, Abel R, Okur A, Strockbine B, Roitberg A and Simmerling C 2006 *Proteins* **65** 712-25
[18] Joung I S and Cheatham T E III 2008 *J. Phys, Chem.* B **112** 9020-41
[19] Ryckaert J-P, Ciccotti G and Berendsen H J C 1977 *J. Comput. Phys.* **23** 327-41
[20] Miller B R, McGee T D, Swails J M, Homeyer N, Gohlke H and Roitberg A E 2012 *J. of Chem. Theory Comput.* **8** 3314-21
[21] Sitkoff D, Sharp K A and Honig B 1994 *J. Phys. Chem.* **98** 1978-88
[22] Flocco M M and Mowbray S L 1994 *J. Mol. Biol.* **235** 709-17
[23] Mitchell J B, Nandi C L, McDonald I K, Thornton J M and Price S L 1994 *J. Mol. Biol.* **239** 315-31
[24] Yokoyama M, Naganawa S, Yoshimura K, Matsushita S and Sato H 2012 *PLoS One* **7** e37530